



Lyman Alpha Galaxies: Primitive Objects, Dusty Starbursts or Evolved Galaxies?

Steven L. Finkelstein, James E. Rhoads, Sangeeta Malhotra (Arizona State University) & Norman Grogin (Space Telescope Science Institute)

Abstract

We present stellar population modeling results for 15 newly discovered Lyman alpha emitting galaxies (LAEs) at $z \sim 4.5$ in the Great Observatories Origins Deep Survey (GOODS) Chandra Deep Field - South (CDF-S). We fit stellar population models to these objects in order to learn specifically if there exists more than one class of LAE. Past observational and theoretical evidence has shown that while many LAEs appear to be young, they may be much older, with Lyman alpha EWs enhanced due to resonant scattering of Lyman alpha photons in a clumpy interstellar medium (ISM). Our results show a large range of stellar population ages (3 - 500 Myr), stellar masses ($1.6 \times 10^8 - 5.0 \times 10^{10} M_{\odot}$) and dust extinction ($A_{1200} = 0.3 - 4.5$ mag), broadly consistent with previous studies. With such a large number of individually analyzed objects, we have looked at the distribution of stellar population ages in LAEs for the first time, and we find a very interesting bimodality, in that our objects are either very young (≤ 15 Myr) or old (≥ 450 Myr). This bimodality may be caused by dust, and it could explain the Lyman alpha duty cycle that has been proposed in the literature. We find that eight of the young objects also require a clumpy ISM to fit their observed SEDs. We find that dust geometry plays a large role in shaping the SEDs that we observe, and that it may be a major factor in the observed Lyman alpha equivalent width distribution in high-redshift Lyman alpha galaxies. We conclude that 13 out of our 15 LAEs are dusty, star-forming galaxies, with the other two LAEs being evolved galaxies.

Introduction

Lyman alpha emitting galaxies (LAEs) were originally predicted to be young, primitive galaxies undergoing copious star formation (Partridge & Peebles 1967). However, a two-phase interstellar medium (ISM) composed of neutral, dusty clumps in an ionized medium could enhance the equivalent width (EW; Neufeld 1991; Hansen & Oh 2006). Because Lyman alpha photons are resonantly scattered, they can escape from this medium, while the continuum photons will suffer extinction and reddening. An evolved stellar population could thus have a large Lyman alpha EW, appearing like a younger galaxy. In Finkelstein et al. (2008a), we analyzed a sample of four LAEs, three of which were best fit by young (5 Myr) dusty ($A_{200} \sim 1 - 2$ mag) stellar populations, similar to those seen by Nilsson et al. (2007) at $z \sim 3.1$ and Pirzkal et al. (2007) at $z \sim 5$. The fourth object was best fit by an old (800 Myr) stellar population, with 0.4 mag of dust in a clumpy ISM, causing significant dust enhancement of the Lyman alpha EW. Further detection of dust-enhancement in a larger sample could help explain the larger than expected EWs seen in many LAEs (e.g., Kudritzki et al. 2000; Malhotra & Rhoads 2002; Finkelstein et al. 2007).

Stellar Population Models

We discovered 11 new LAEs at $z \sim 4.5$ in the CDF-S using narrowband imaging with MOSAIC II at the CTIO Blanco 4m telescope. We compared observations to stellar population models, using the public GOODS *HST*, *Spitzer*, and VLT/ISAAC data. We computed model stellar population spectra using the software from Bruzual & Charlot (2003), with a grid of metallicities, star formation histories (SFHs), and stellar population ages. We also included Ly α emission lines, calculated from the number of ionizing photons. We applied dust via the dust law from Calzetti et al. (1994). When dust was applied to a continuum wavelength element, we multiplied the flux by $e^{-\tau}$. For the Ly α wavelength bin, we instead multiplied by $e^{-\tau}$, where q is the clumpiness parameter, which ranged from 0 (EW enhanced) to 10 (EW suppressed). The important point is that for any value of $q < 1$, the Ly α EW is being enhanced over that intrinsic to the star forming regions. All of our models were redshifted corresponding to the central wavelength of the detection filter, and then attenuated by Madau (1995) intergalactic medium absorption.

Results

Figure 3 shows the best-fit models to each candidate LAE, as well as the best-fit model with a two-burst SFH (one maximally old burst, and one burst at any time). The last two columns show the results of 7000 Monte Carlo simulations, which we used to estimate how well the best-fit model constrains the given object.

In Figure 4a we show the distribution of best-fit ages from our models. Most objects have ages ≤ 15 Myr, with three out of the 15 objects showing ages ≥ 40 Myr. However, we see a large age gap, from 50 - 450 Myr. In Figure 4b we show the distribution of the best-fit clumpiness parameter, finding that 60% (9/15) of our objects require an ISM dominated by a clumpy geometry ($q < 1$). Our derived masses span 8.4×10^7 to $6.0 \times 10^9 M_{\odot}$, with half of our sample at or over $10^9 M_{\odot}$. These results are similar to those seen in past studies (Gawiser et al. 2006; Pirzkal et al. 2007; Lai et al. 2007, 2008), which range from 7×10^7 to $1.4 \times 10^9 M_{\odot}$. We also find a slight trend toward lower metallicity, as 8/15 objects have $Z \leq 0.02 Z_{\odot}$.

The presence of dust in every LAE is interesting, although many other studies have found evidence for dust extinction as well. While Lai et al. (2008) and Gawiser et al. (2006) do not find dust in their stacking analyses (Nilsson et al. (2007) do find dust in their stacking analysis), Chary et al. (2005), Pirzkal et al. (2007) and Lai et al. (2007) do find dust in their analyses of individual objects, with A_{λ} as high as $1.3 (A_{1200} \sim 4 \times A_{\lambda})$. To measure the average properties of our sample, we averaged the fluxes in each band from our best-fit models, and then re-fit this "stack" of our objects. We found that our sample has an average stellar population with $t_{\text{exp}} = 6$ Myr, $8.0 \times 10^8 M_{\odot}$, $A_{1200} = 2.5$, $q = 1$ and EW $\sim 90 \text{ \AA}$, with a 99% confidence level of containing some measure of dust.

Table 1: Best-fit results for all 15 objects. If a given object's best-fit point does not lie in its largest 68% confidence Monte Carlo contour, we assign the object a "most-likely" model, derived from the center of the largest 68% contour. These values are shown in parenthesis.

| Name | t_{exp} (Myr) | Mass ($10^8 M_{\odot}$) | Z | Z_{SFH} (yr) | A_{1200} (mag) | q | Model EW (\AA) | χ^2 |
|-------|------------------------|---------------------------|-------|-----------------------|------------------|-------------|---------------------------|----------|
| CHa-1 | 3.0 | 28.12 | 0.2 | 4×10^7 | 1.00 | 2.00 | 81.49 | 0.52 |
| CHa-2 | 50.0 (4.0) | 135.53 (52.84) | 0.02 | 10^8 | 1.25 (2.00) | 1.00 (1.00) | 75.54 | 0.51 |
| CHa-3 | 453.5 | 383.94 | 0.2 | 4×10^9 | 0.30 | 0.00 | 97.43 | 0.32 |
| CHa-4 | 6.0 | 58.28 | 0.005 | 10^7 | 1.00 | 3.00 | 27.39 | 1.94 |
| CH8-1 | 2.5 (12.0) | 29.16 (157.11) | 1.0 | 10^7 | 2.00 (4.00) | 1.00 (0.25) | 131.32 | 0.93 |
| CH8-2 | 10.0 | 45.72 | 0.005 | 10^7 | 0.50 | 5.00 | 20.04 | 1.07 |
| CS2-1 | 13.2 | 128.93 | 0.02 | 10^7 | 2.50 | 0.75 | 135.83 | 9.60 |
| CS2-2 | 13.2 | 205.40 | 0.005 | 10^8 | 3.50 | 0.00 | 398.16 | 2.23 |
| CS2-3 | 12.0 | 605.09 | 0.005 | 10^8 | 4.50 | 0.25 | 340.76 | 0.74 |
| CS2-4 | 4.0 (500.0) | 100.86 (4972.0) | 0.005 | 10^8 | 5.00 (3.50) | 0.75 (0.00) | 478.33 | 0.82 |
| CS2-5 | 15.1 | 16.74 | 1.0 | 10^7 | 1.00 | 0.00 | 122.85 | 3.28 |
| CS2-6 | 40.0 (7.0) | 476.58 (94.79) | 1.0 | 10^7 | 4.00 (4.50) | 0.00 (0.00) | 999.58 | 0.07 |
| CS2-7 | 5.0 | 276.76 | 0.005 | 10^8 | 3.00 | 1.50 | 30.58 | 2.39 |
| CS2-8 | 5.0 | 16.08 | 1.0 | 10^7 | 3.00 | 0.00 | 533.27 | 1.47 |
| CS2-9 | 13.2 (7.0) | 8.39 (32.85) | 1.0 | 4×10^9 | 0.80 (3.00) | 0.00 (0.00) | 140.79 | 0.01 |

Figure 1: PEARs spectra of CHa-2, showing signs of a Lyman break and Lyman alpha line at the expected wavelengths for $z \sim 4.5$. PEARs spectra confirmed the redshifts of three of our candidate LAEs.

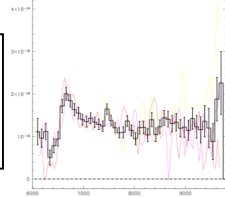


Figure 2: Stamps of our 11 new candidates in the narrowband, HST ACS and Spitzer IRAC images.

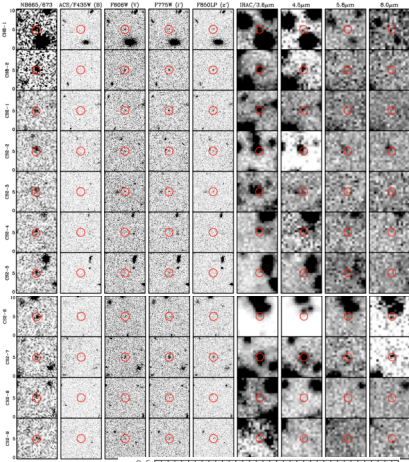
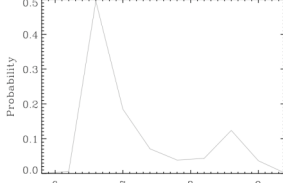


Figure 5: Average age probability curve for our entire sample using the results from the Monte Carlo simulations.



Discussion

Figure 5 shows the average age probability distribution of our sample, derived from the Monte Carlo results. This figure verifies Figure 4a, as we see two distinct peaks in age, at 4 Myr and 400 Myr. LAEs residing in the larger peak appear to all be dusty, star-forming galaxies, while those in the older peak are evolved galaxies. There are many scenarios one could think of to fit this distribution. Perhaps the distribution of ages is continuous, and we just need a larger sample to fill in the gaps. One intriguing possibility is that this distribution is true, i.e. we see Ly α galaxies when they are very young, but then some physical mechanism is blocking the Ly α emission until much older age. Before the first generation of stars dies, Ly α photons may find it easier to escape (especially if the initial ISM is clumpy). After 10-20 Myr, stars will begin to die, and these young galaxies will get dustier. As the dust gets thicker, the amount of Ly α escaping will be reduced. However, after some period of time, the stars may begin to "punch holes" through the dust, resulting in a clumpy (or hole-y) ISM that can enhance the observed EW, creating objects like CHa-3 and CS2-4. This age bimodality could explain the Ly α duty cycle proposed in the literature (e.g., Shapley et al. 2001).

Figure 4:

- (a) Histogram of best-fit ages.
- (b) Histogram of best-fit clumpiness parameters.

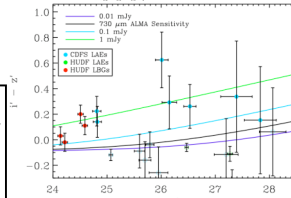
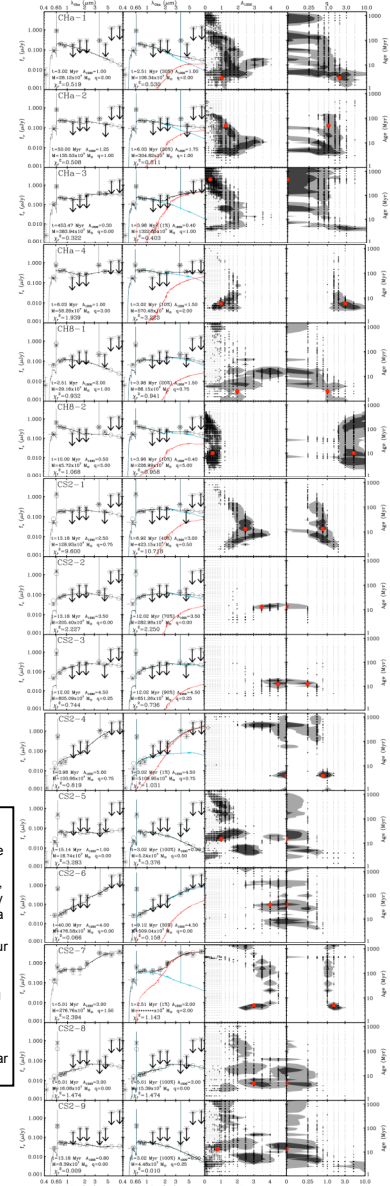


Figure 6: Comparing LAEs to ALMA's sensitivity, we find that 47% of our sample should be seen with ALMA.

Future Studies

Our detection of dust in all of our LAEs leads to interesting ideas for the future. We have derived the level of dust via its effect on the rest-UV spectrum. However, this reddening is degenerate with the age, thus we could better constrain the amount of dust by detecting dust emission directly. Using the Atacama Large Millimeter Array (ALMA) as a test for future observatory capability, we found that 47 \pm 20 % of our LAEs would be detected with ALMA if they had at least as much dust as we derived in this study (Finkelstein et al. 2008c). We did this by computing their rest-frame FIR flux using the FIR - β relation from Meurer et al. (1997). The figure below on the left shows the results from this study. Knowing *a priori* the level of dust will improve the fidelity of stellar population modeling results.

Figure 3: Results from model fitting. From the left: Best-fit single population model; Best-fit two-burst model; Age vs. A_{1200} Monte Carlo results; Age vs. q Monte Carlo results.



Selected References

Finkelstein et al. 2007, ApJ, 660, 1023
Lai et al. 2007, ApJ, 655, 704
Finkelstein et al. 2008a, ApJ, 678, 655
Malhotra & Rhoads 2002, ApJ, 565, L71
Finkelstein et al. 2008b, ApJ submitted
Meurer et al. 1997, AJ, 112, 54
Finkelstein et al. 2008c, MNRAS submitted
Neufeld 1991, ApJ, 370, 85
Nilsson et al. 2007, A&A, 471, 71
Hansen & Oh 2006, MNRAS, 367, 979
Shapley et al. 2001, ApJ, 562, 95